# APPLICATION OF COMPUTATIONAL FRACTURE MECHANICS TO REPAIR OF LARGE CONCRETE STRUCTURES

A. Ingraffea, B. Carter, P. Wawrzynek
Cornell Fracture Group, Cornell University
Ithaca, New York, U.S.A.

## Abstract
Computational linear elastic fracture mechanics can be used for relatively large concrete structures as a quantitative guide in:
- forensic engineering: the use as a primary diagnostic tool in determining the cause of cracking;
- repair of cracked structure: the use in the design of cost-effective and safe repair procedures.

Two examples are given of the latter use. In the first, linear elastic computational fracture mechanics is used to decrease the probability of crack growth caused by pressure injection of grout into a crack in a doubly curved arch dam. In the second, it is used to design a post-tensioned retrofit of a bridge plinth to decrease stress intensity on existing or possible future cracks.

# 1  Introduction

Computational fracture mechanics (CFrM) can be applied to concrete structures as a tool for:

- forensic engineering: use as a primary diagnostic tool in determining the cause of cracking.
- repair of cracked structure: use in the design of repair procedures for cracked structures.

Much of the work in the application of fracture mechanics to large concrete structures falls into the first category and was inspired by the landmark work of Cloug65 on finite element analysis, without fracture mechanics, of cracking in a concrete gravity dam. Examples include investigations into the cause of cracking in the Fontana gravity dam [Chapp81, Ingra90], the Kölnbrein doubly curved arch dam [Linsb89], and the Schoharie Creek Bridge [Swens91].

The focus of the present paper, however, is on the second category. Because we will investigate repair of relatively large structures, we will use linear elastic fracture mechanics (LEFM) to design schemes to:

- decrease the level of stress intensity on existing cracks;
- arrest stable crack growth;
- decrease the probability of crack growth caused by repair procedures.

All of these capabilities will be herein illustrated through computational examples based on possible repair procedures of actual structures, one dam and one bridge plinth.

To be useful and practical for the solution of repair problems, computational LEFM should be able to represent actual crack geometries found or expected in the structure. This means that the crack geometry cannot be restricted by the discretization method or by assumptions imposed by any calculation procedure. Next, the computational procedure itself should be able to capture all of the relevant physics of the problem, including coupling with thermal or fluid processes, to determine accurately all of the stress intensity factors for all modes present. Finally, the method should be able to remesh automatically the new geometry which occurs with each increment of crack growth. All of these capabilities have been designed into FRANC2D [Bitte95] and FRANC3D [Marth93], the programs which will be used to perform the examples to follow.

## 2 Example problems

### 2.1 Example I: grout pressure control in a dam

In this example we show how computational LEFM can be used to control a common crack repair procedure in concrete dams, pressure grouting. The objective in this procedure is to completely fill an existing crack by injection of grout, while assuring that the pressures generated in the crack by the process do not cause further extension of the crack. The key variables in the design of the repair procedure are grout injection viscosity, injection rate, pressure, and time, and number of injection points. Currently, judgment and experience are used to try to optimize these variables.

What is proposed here is a rationalization of the process based on:
* better knowledge of the crack geometry;
* capability for simulation of coupled fluid-flow and stress analysis;
* capability to compute stress intensity along the existing crack front as a function of the above-mentioned variables.

Current research into the state-of-the-art impact echo method [Sansa89] shows promise for being able to locate and determine the shape of existing cracks in dams. This example will show, for a hypothetical repair procedure on an actual dam, the later two capabilities.

Figure 1 shows the model used for this example. It is one of an existing doubly-curved arch dam with a maximum height of 135 m. This dam has been previously studied in Marth91 and in Llorc87. The mouth of the existing non-symmetrical crack can be seen about mid-height on the upstream face.

The fluid flow capability in FRANC3D was designed specifically for hydraulic fracture simulation. The elasticity, lubrication, and mass balance equations are combined, leading to a unique solution for fluid pressure distribution and aperture near the crack front [Desro94]. The fluid pressure obtained form the flow equations is coupled with the elastic structural response through a set of influence functions that are linearly combined to give the displacements at the crack front [Sousa93]. The number of injection points, injection flow rate, fluid viscosity, and pumping time can all be varied, leading to different fluid pressure distributions and crack opening displacements. The numerical objective is to find a unique solution where $K_I$ equals $K_{Ic}$ and the fluid speed matches the crack propagation speed.

Injection points are located at the mouth of the crack on the upstream face, where grout with a specified initial viscosity will be injected at a constant flow rate for each simulation. It is assumed
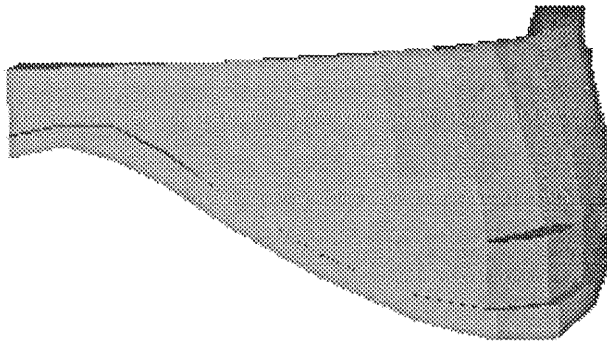
Fig. 1. FRANC3D solid model of the doubly curved arch dam with crack originating from upstream face. From Marth91.

that the repair procedure is taking place under empty reservoir conditions so that the only other loading on the dam is self-weight.

The focus of this example is to show the effects of variation of the injection rate, number of injection points, and injection time on stress intensity, with injection viscosity constant for all simulations. Three injection rates and times, and one and three injection points were used in simulations which produced the results shown in Figures 2 through 4. Figure 2 shows a plan view of a typical pressure distribution in the crack early in the process of injection from three points, before coalescence of the grout front has occurred. Figure 3 shows a typical pressure distribution just after complete filling of the crack has occurred.

The coupled analysis produces injection-time-dependent distributions of $K_I$, $K_{II}$, and $K_{III}$ along the existing crack front. Figure 4 shows a typical $K_I$ distribution obtained during injection from three points. The results are summarized in Table 1. The numbers in parentheses in the injection rate column indicate the number of injection points used.

Results such as those shown in Table 1 can be used to optimize the repair process. The number of injection points and the volume of grout and maximum pump pressure needed are key variables in the cost of the repair. The maximum $K_I$ is the key variable in minimizing the likelihood of grouting-induced additional cracking. For example, in all of the cases considered here, the maximum $K_I$ occurs at the tips of the crack mouth on the upstream face of the

Table 1. Results from simulation of grout injection,
grout viscosity, μ= 0.001 MPa s

| Injection Time (min.) | Total Injection Rate (X 10^3 m^3/s) | Max KI (MPa √(m)) | Grout Volume (m^3) | Max Pressure (MPa) |
|---|---|---|---|---|
| 0.38 | 90 (3) | 12.5 | 2.07 | 7.26 |
| 2.45 | 30 (1) | 8.5 | 4.41 | 6.57 |
| 69.50 | 0.9 (3) | 5 | 3.75 | 2.93 |
| 264.28 | 0.3 (1) | 4 | 4.76 | 2.49 |

dam. This is valuable information because these locations are usually visible during grouting, and therefore can be used as a check on the safety of the repair process.

Clearly, other design parameters, such as grout viscosity or variable location of the injection points, could also be accommodated within this simulation environment. The main point here is that the use of computational LEFM, in the form of stress intensity factor control, can be used to design an effective and safe grout injection repair procedure.

## 2.2 Example II: design of post-tensioned retrofit in a bridge plinth

In this example we describe a hypothetical retrofit procedure for a class of unreinforced bridge plinth. The origin of the problem was the failure of the Schoharie Creek bridge on the New York State Thruway in 1987. A complete non-linear fracture mechanics analysis of this failure was reported in Swens91.

Figure 5 shows an elevation view of one of the bridge piers. Although the columns and tie beam are heavily reinforced, only shrinkage and temperature steel were included in the original design of the plinth. The failure of the Schoharie Creek bridge was caused by fracture of a pier of this type, induced by scour resulting from a record flood. Figure 6 is a photograph of the failed plinth.

Because a relatively large number of bridge piers of this type are still in service in the US, a retrofit which would reduce the likelihood of a similar failure should be used. In this example, we will use computational LEFM to design a retrofit based on post-tensioning the plinth.

About one year after the opening of the Schoharie Creek bridge, nearly vertical cracks were observed, see Figure 7, in the plinths of its piers, originating approximately at point B in Figure 5. These cracks were attributed to excessive tensile stress along the top of the
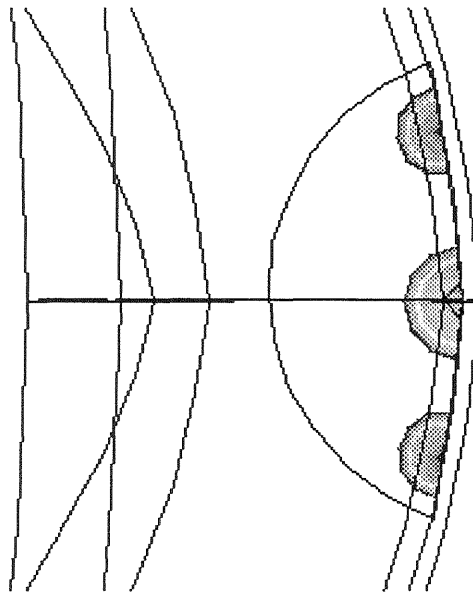
Fig. 2. Grout pressure distribution in the crack. Three injection
points, time is 10 min.
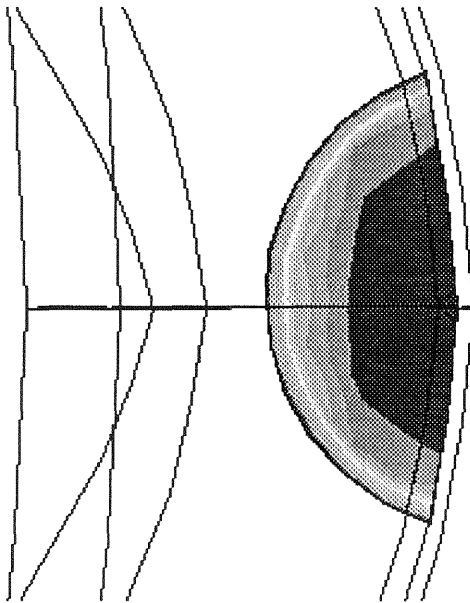


Fig. 3. Grout pressure distribution in the crack. Maximum pressure
is 2.93 MPa, three injection points, time is 69.5 min.
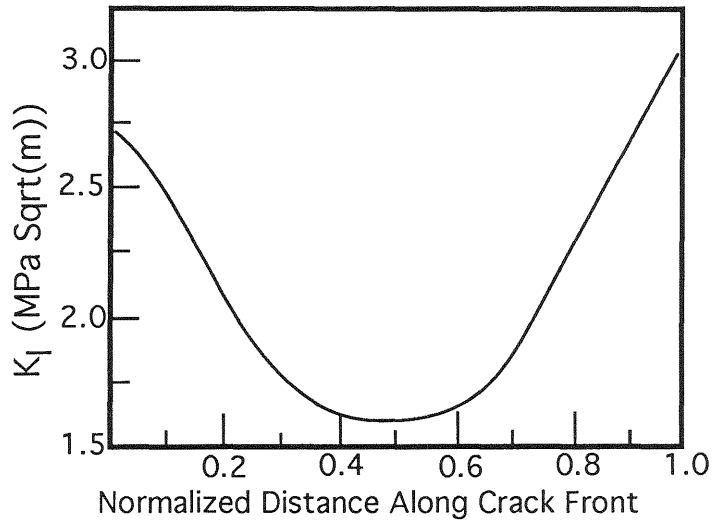
Fig. 4 Distribution of $K_I$ along the crack front, three injection points, $9 \times 10^{-4}$ m$^3$/s total injection rate, 30 minutes injection time.
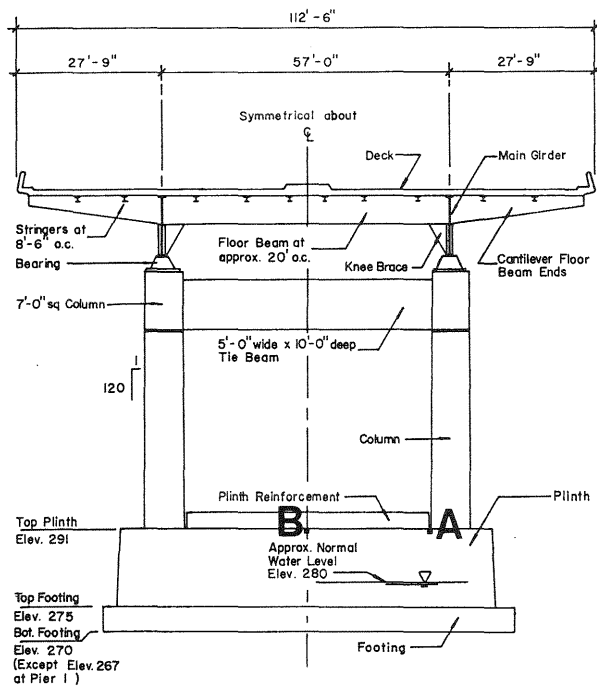


Fig. 5. Configuration of typical pier showing plinth reinforcement and initiation points for cracking. After Wiss87.
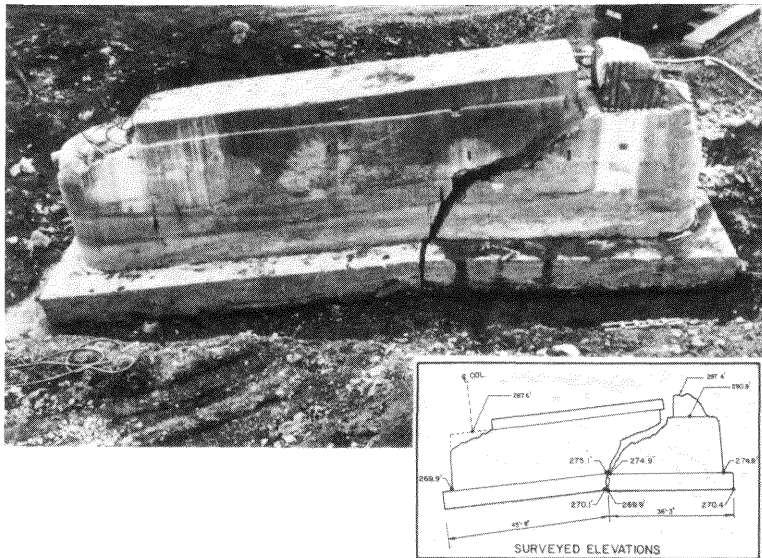
Fig. 6. Photograph of failed plinth. From Wiss87.
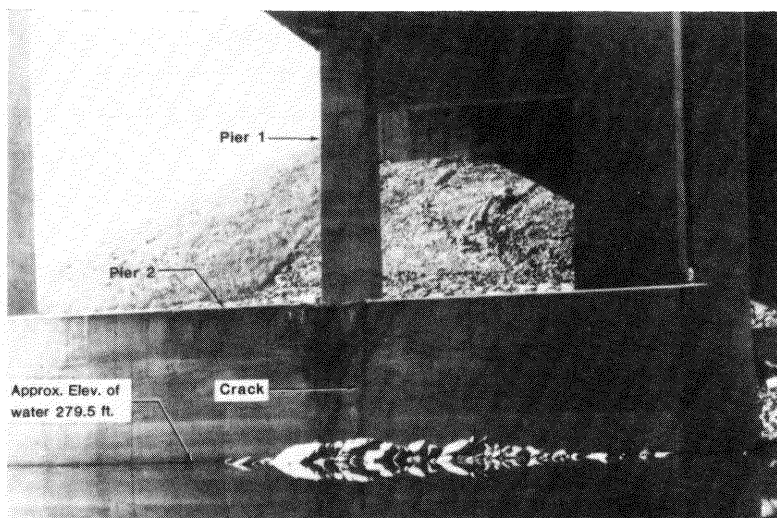


Fig. 7 Crack originating from top of plinth, soon after start of
service. From Wiss87.

plinth due to support pressures on the base of the footing. The plinth
reinforcement shown in Figure 5 was then added as a retrofit.
Swens91 explain how this retrofit repaired the observed cracking,
but, because it was not continuous across the entire length of the
plinth, could not inhibit the type of fracture originating at Point A in
Figure 5, and shown in Figure 6. In fact, the additional stress

concentration caused by the notch created around Point A by this repair procedure exacerbated the problem.

An alternative retrofitting procedure, designed using fracture mechanics, will be described here. It consists of the addition of post-tensioned tendons, either connected externally or ducted through the plinth, at a level of 1.5 ft (0.46 m) below the top of the plinth. The design objective is that the magnitude on the horizontal compressive force to be supplied by these tendons must be sufficient to keep $K_I$ equal to zero for any length of crack which might initiate from points A or B.

FRANC2D was used to propagate cracks from both points along trajectories dictated by the boundary conditions. For propagation from Point A, driven by dead and live load and by scour over one-half of the length of the plinth, the trajectory was curvilinear, as shown in Figure 8. For propagation from Point B under symmetrical dead and live load only, the trajectory was self-similar as shown in Figure 9. These computations produce stress intensity vs. crack length histories as shown in Figure 10. The stress intensities caused by a 1 kip (4.45 kN) post-tensioning force applied as described above were also computed during these crack growth simulations, Figure 11.

As an example of repair design using this information, consider a situation in which a 60 in. (1.52 m) long crack, due to dead and live load, is discovered originating from Point B, similar to the actual occurrence shown in Figure 7. From Figure 10 one can obtain a $K_I$ of about 1.7 ksi√in (2 MPa√m) due to these loadings on this crack. From Figure 11 one can obtain a $K_I$ of about $-1.5 \times 10^{-3}$ ksi√in (-1.7 kPa√m) for a 1 kip ( 4.45 kN) post-tension force. The required post-tension force, $F^{pt}$, to just bring $K_I$ equal to zero for this situation would be approximately,

$$F^{pt} = 1.7/(1.5 \times 10^{-3}) = 1{,}133 \text{ kips (5.1 MN)} \qquad (1)$$

The same figures can be used for a situation where the same length crack is discovered originating from Point A, due to scour over one half the length of the plinth. In this case, the required post-tension force would be approximately,

$$F^{pt} = 5.9/(1.7 \times 10^{-3}) = 3{,}470 \text{ kips (15.4 MN)} \qquad (2)$$
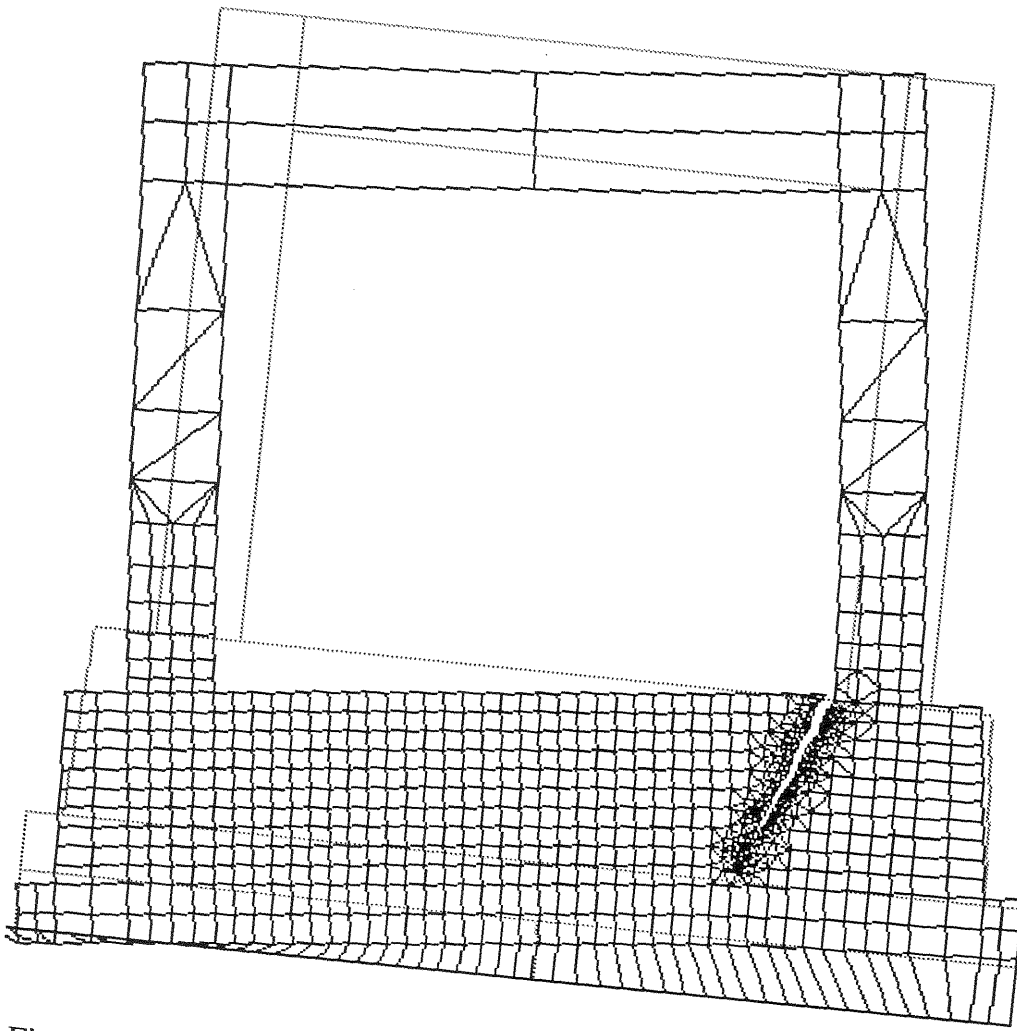
Fig. 8. Final deformed finite element mesh after fourteen 1 ft (0.30 m) increments of predicted cracking from Point A. Dead and live load, and 41 ft (12.5 m) of scour. Magnification factor is 25.

A functional relationship between the required post-tensioning force and the target crack length can be easily developed from the data shown in Figures 10 and 11.

## 3  Conclusions

Linear elastic computational fracture mechanics can be used as a quantitative guide to the repair of relatively large cracked concrete
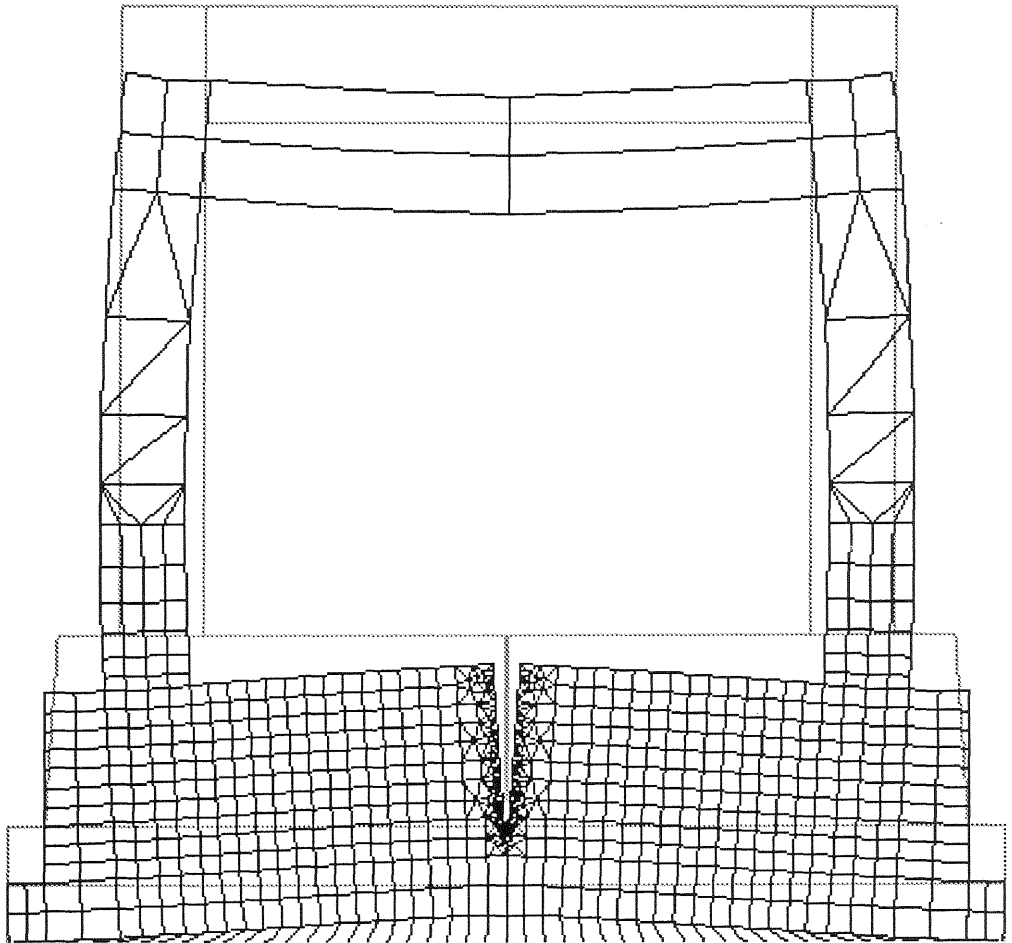
Fig. 9. Final deformed finite element mesh after fourteen 1 ft (0.30 m) increments of predicted cracking from Point B. Dead and live load only. Magnification factor is 500.

structures. Two examples were given of this use. In the first, a three dimensional, coupled fluid flow/solid stress analysis technique is used to compute stress intensity factors along the front of a crack in a doubly curved arch dam due to pressure injection of grout in the crack. This information can be used to optimize the grout treatment, and to decrease the probability of crack propagation due to the grouting pressures. In the second example, stress intensity factor histories are computed for cracks originating at two locations in a plinth supporting a highway bridge. These cracks can be due to dead and live loads, or to unexpected flood-related damage. This information is then used to design a post-tensioning scheme to retrofit plinths which have, or could have such cracking.
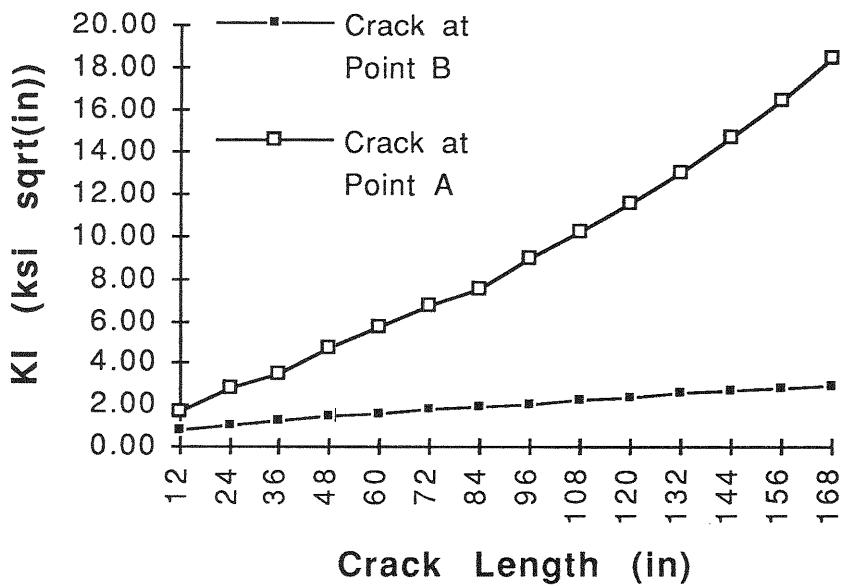
Fig. 10. Computed $K_I$ due to dead plus live load only.
(1 in = 25.4 mm, 1 ksi√in = 1.12 MPa√m)
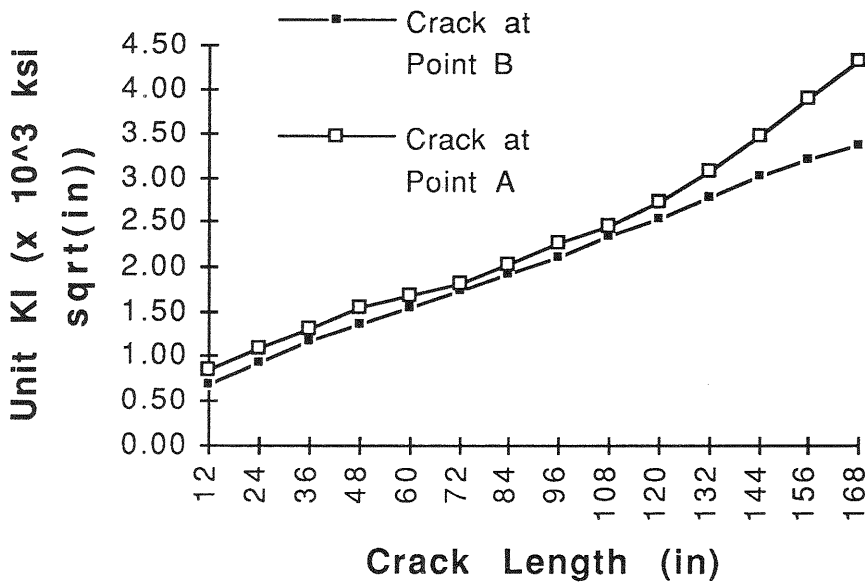


Fig. 11. Computed $K_I$ due to 1 kip (4.45 kN) post-tensioning force,
with 41 ft (12.5 m) of scour.

# 4 References

Bittencourt, T., Sousa, J., Wawrzynek, P., Ingraffea, A. R. (1995) Quasi-automatic simulation of crack propagation for 2D LEFM problems. to appear in **Eng. Fract. Mech.**

Clough, R. W., Tocher, J.L. (1965) Analysis of thin arch dams by the finite element method, in **Proc. Symp. on Theory of Arch Dams**, Pergamon Press, Oxford.

Chappell, J. F., Ingraffea, A. R. (1981) A Fracture mechanics investigation of the cracking of fontana dam. **Department of Structural Engineering Report 81 - 7**, School of Civil and Environmental Engineering, Cornell University, Ithaca, N.Y.

Desroches, J., Detournay, E., Lenoach, B., Papanastasiou, P., Pearson, J., Theircelin, M., Cheng, A. (1994) The crack tip region in hydraulic fracturing. **Proc. Royal Soc. London**, A, 1447, 39-48.

Gaisbauer, H. R., Ingraffea, A. R., Rossmanith, H. P., Wagner, E. (1990) Bruchmechanische Überlegungen bei gewölbesperren, in **Proceedings of the 6th International Seminar on Hydraulic Structures**, Vienna, 215-230.

Ingraffea, A. R., Linsbauer, H.N., Rossmanith, H.P. (1987) Computer simulation of cracking in a large arch dam: downstream side cracking, in **Fracture of Concrete and Rock** (eds. S. Shah and S. Swartz) Springer Verlag, New York, 334 - 342.

Ingraffea, A. R. (1990) Case studies of simulation of fracture in concrete dams. **Engineering Fracture Mechanics**, 35, 1/2/3, 553-564.

Linsbauer, H. N., Ingraffea, A. R., Rossmanith, H. P., Wawrzynek, P. A. (1989) Simulation of cracking in a large arch dam: Part I. **Journal of Structural Engineering**, 115, 7, 1599 - 1615.

Linsbauer, H. N., Ingraffea, A. R., Rossmanith, H. P., Wawrzynek, P. A., (1989) Simulation of cracking in a large arch dam: Part II. **Journal of Structural Engineering**, 115, 7, 1616 - 1630.

Llorca, J., Elices M., and Ingraffea, A. R. (1987) Analisis lineal y no lineal de propagacion de fisuras en hormigon, **Revista Internacional de Metodos Numericos para Calculo y Diseno en Ingenieria**. 3, 3, 309 - 333.

Martha, L.F., Llorca, J., Ingraffea, A. R., and Elices, M. (1991) Numerical simulation of crack initiation and propagation in an arch dam. **Dam Engineering**, 2, 3, 193-214.

Martha, L., Wawrzynek, P., Ingraffea, A. R. (1993) Arbitrary crack propagation using solid modeling. **Engineering with Computers**, 9, 2, 63-82.

Sansalone, M., Carino, N. (1989) Detecting delamination in concrete slabs with and without overlays using the impact echo method. **Materials J. Amer. Conc. Inst.**,86, 175-184.

Swenson, D. V., Ingraffea, A. R. (1991) The collapse of the Schoharie Creek bridge: A case study in concrete fracture mechanics. **Int. Journal of Fracture**, 51, 73-92.

Stauble, H., Wagner, E., Rossmanith, H., Ingraffea, A. (1991) Cracking of boreholes in arch dams due to high pressure grouting, in **Proc. of the Int. Conf. Dam Fracture**, ( eds. V. Saouma, R. Dungar, D. Morris), Electric Power Research Institute, GS-7491, 589-604.

Sousa, J., Carter, B., Ingraffea, A.(1993) Numerical simulation of 3D hydraulic fracture using Newtonian and power-law fluids. **Int. J. Rock. Mech. Mun. Sci. & Geomech. Abstr.**, 30, 1265-1271.

Wiss, Janney, Elstner Assoc. Inc. and Meuser Rutledge Consulting Engineers (1987) Final Report, Collapse of the thruway bridge at Schoharie Creek. New York State Thruway Authority, Albany, New York.